

The Impact of Directional Antenna Models on Simulation Accuracy

Eric Anderson, Gary Yee, Caleb Phillips, Douglas Sicker, and Dirk Grunwald

Department of Computer Science
University of Colorado
Boulder, Colorado, USA

Email: {eric.anderson,gary.yee,caleb.phillips,sicker,grunwald}@colorado.edu

Abstract—Increasingly, directional antennas are being used in wireless networks. Such antennas can improve the quality of individual links and decrease overall interference. However, the interaction of environmental effects with signal directionality is not well understood. We observe that state of the art simulators make simplifying assumptions which are often unrealistic and can give a misleading picture of application layer performance. Because simulators are often used for prototyping and validating new ideas, their realism and accuracy are of primary importance. In this paper, we apply a new empirical simulation method for directional antennas and study how well this models reality. We show that not only is our model easy to implement, but is also more accurate and thus better able to predict the performance of propagation-sensitive applications.

I. INTRODUCTION

Using directional antennas is currently one of the main techniques for improving link quality by increasing signal strength in some directions while lowering interference in others. Many directional networking protocols and applications, however, are studied using wireless simulation models that assume directional antennas experience environmental effects in the same way that omnidirectional antennas do. This, in turn, influences the expected behavior of the entire network stack, potentially producing significant discrepancies between simulations and empirical results.

This work makes the following contributions to improve the fidelity of wireless network simulators:

- We show that current state of the art techniques do not accurately capture the effects of the environment on directional signal propagation and can thus produce misleading results at higher layers of the network stack.
- We introduce an empirically derived model for *signal directionality*, the *Effective Directivity Antenna Model* (EDAM), that incorporates the environment’s effects on directional antennas as a stochastic process.
- We verify EDAM’s accuracy as a simulation technique by using it to model a data-striping application where the physical boundaries of successful packet reception are critical to overall success.
- We perform real-world indoor and outdoor experiments and compare the results with those obtained by various

simulation techniques. We find that simulation based on EDAM can improve fidelity by about 60%.

In the next section, we discuss related work. In section III, we discuss our proposed simulation approach and the model on which it is based. Section IV presents a security-oriented smart-antenna application as a case study. We discuss its implementation, simulation, and an analysis of the accuracy of the various simulation approaches. Finally, in section V, we conclude.

II. BACKGROUND AND RELATED WORK

In this section, we discuss the state of the art with respect to the way network simulators model the physical layer. Figure 1 shows the simulation framework we conceptualize in this work. We argue that while path loss models and fading models capture some of the vagaries of the medium, they insufficiently model the effects of the environment on signal directionality. Additionally, prior work [1] has shown that the way the physical layer is simulated can have substantial effects on higher layer results. This motivates our work into building an empirically derived model for the environmental effects on antenna directionality, which we call a “directivity model” and can be used in combination with fading and path loss models to produce a more realistic simulation of the physical layer effects in systems where antenna directionality plays a role.

Wireless network simulators use a *path loss model* to model the degradation of a transmitted signal. In free space, energy is propagated in all directions and the energy that actually strikes the receiver is proportional to the square of the distance between the transmitter and receiver – the signal is attenuated $\propto r^2$. This, however, ignores significant effects found in terrestrial environments. Of particular concern are absorption and refraction by obstacles and *multipath interference*, where the radio frequency (RF) waves bounce off objects in the environment and converge at the receiver after traversing different distances (and thus potentially out of phase.)

The commonly-used “two-ray” path-loss model uses a reflection from the earth and the heights of the transmitter and receiver to indicate the likely signal strength at a given distance. Other models for such effects are based on fitting empirical measurements rather than *a-priori* analysis. There are

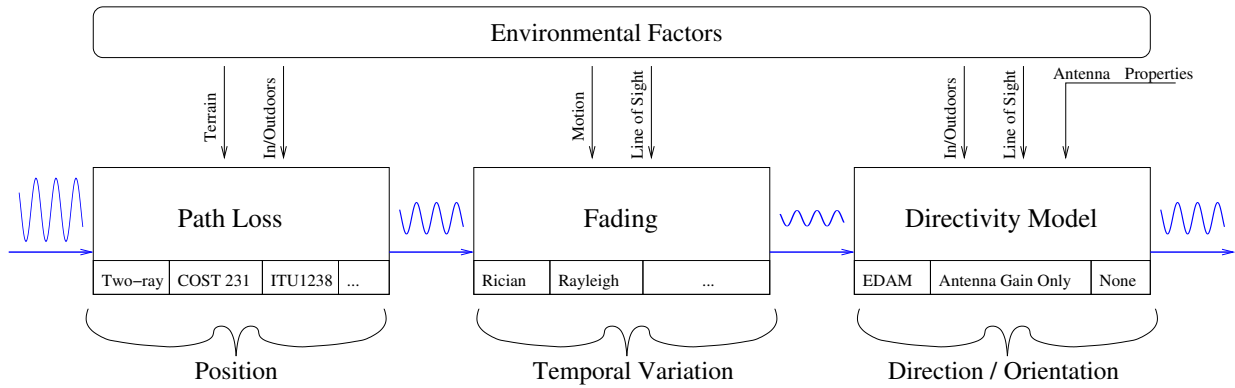


Fig. 1: Physical-layer simulation framework.

general-purpose models such as the Hata / COST231 model and the Longley-Rice model [2], [3], and several specific to the wavelength and operating characteristics of wireless LAN cards [4]. Additionally, the propagation characteristics of indoor environments are sufficiently different from outdoors that there are a number of measurement studies and models (see [5], [6] and [7] for excellent surveys).

The preceding models describe relatively large-scale phenomena. In addition to whatever long-range attenuation there may be, there is also *small-scale fading*, which is the result of multipath interference and occurs at the scale of single wavelengths. While this can theoretically be predicted analytically, it would require that the environment be known with a level of detail that is generally impractical [8], [9]. A common way of addressing such situations is through *statistical fading* models. Rather than determine the signal strength at any exact place or time, it is modeled as a random variable with a known distribution. In general, the distributions are fairly well-established, but the parameters are environment-specific (see e.g. [10]). There are several common models, among them *Rayleigh fading*, which assumes that there are many comparable multipath signals, and *Ricean fading*, which assumes a less “cluttered” environment in which line-of-site paths are more important.

The concern addressed by this paper is that those models do not consider an environmental component to directivity. Our model for directional antennas adopts a similar approach to the empirical path-loss and statistical fading models – we use empirical measurements to identify the characteristics of the random or stochastic process. Where we differ is that our model is primarily concerned with effects on directionality.

The most commonly used simulators in networking research (OPNET, QualNet, and NS-2) do not consider antenna directionality and radio propagation as interacting variables. Each one supports several models of path loss, and possibly fading, but they all follow the same general model with regard to antenna gain: For any two stations i and j , the received signal strength is computed according to the general form of

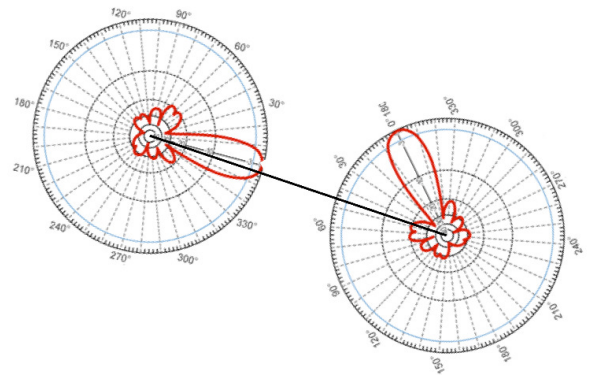


Fig. 2: Standard simulation modeling of directional antennas assume all signals are emitted along a single path.

equation 1:

$$\text{Received Power} = P_{tx} * G_{tx} * L(i, j) * G_{rx} \quad (1)$$

The received power P_{rx} is the product of the transmitted power P_{tx} , the transmitter’s gain G_{tx} , the path gain (loss) $L(i, j)$ between the two stations, and the receiver’s gain G_{rx} . The transmitter and receiver gains are essentially constants in the case of omnidirectional (effectively isotropic in the azimuth plane) antennas. For directional antennas, gain is an antenna-specific function of the direction of interest. For some given zenith ϕ , azimuth θ , and an antenna-specific characterization function $f_a(\cdot)$, the power transmitted in that direction is given by equation 2:

$$\text{Gain in direction } (\phi, \theta) = f_a(\phi, \theta) \quad (2)$$

$$\text{Combined gain} = f_a(\phi, \theta) * f_b(\phi', \theta') \quad (3)$$

Correspondingly, the receiver gain is modeled by a (potentially different) function $f_b(\cdot)$ of the direction from which the signal is received.

The above models describe the power emitted in or received from a single direction (see figure 2). In reality, *the transmitter’s power is radiated in all directions, and the receiver*

aggregates power (be it signal or noise) from all directions. Besides being a source of interference for a dominant signal, the energy traveling along secondary paths (due to side lobes) also carries signal. Network simulators model the antenna gain and path loss using the angles and straight-line distance between the transmitter and receiver. However, if one of the “secondary” reflected or refracted signal paths is aligned with a high-gain direction of a transmitting or receiving antenna, the received power from that path can be greater than that of the “primary” path. Thus in environments with significant multipath, the gain cannot be determined based solely on a single direction. It makes intuitive sense that if a narrow beam is directed into a scattering environment, the resulting signal is probably not narrowly focussed.

Although the simulators we are considering assume that the single direction of interest for each station is precisely toward the other station, one can generalize equations 1 and 3 to the case where there are multiple significant signal paths. In this case, it is crucial to note that f_a , f_b , and L_l are complex, so summation does not automatically imply an *increase* in magnitude.

$$P_{rx} = \sum_{l \in \text{paths}} P_{tx} * f_a(\phi_l, \theta_l) * L_l(i, j) * f_b(\phi'_l, \theta'_l) \quad (4)$$

This assumes that there is some way to identify the available paths that a signal may take. As with the Rayleigh and Ricean fading models, it may be possible to build a parameterized model of the cumulative effect of those paths for “cluttered” and “uncluttered” environments.

III. A NEW SIMULATION APPROACH

In [11], we present a statistical model for the environmental effects on antenna directionality. This statistical model can be used as the basis for more realistic simulations. It has long been recognized that radio propagation involves very environment-specific effects. We identify three major ways of addressing such effects in modeling and simulation: The first is to simply ignore the variability and use a single representative value in all cases. The second, which goes to the opposite extreme, is to model specific environments in great detail. A third approach is to randomly generate values according to a representative process and perform repeated experiments.

Each approach has its benefits, but we are advocating the repeated-sample approach. Precisely modeling a specific environment probably has the greatest fidelity, but it provides no information as to how well results achieved in a single environment will generalize to others. Stochastic models have the advantage of being able to produce arbitrarily many “similar” instances, and parametric models make it possible to study the impact of varying a given attribute of the environment. Such approaches are frequently used to model channel conditions [6], network topology [12], [13], and traffic load [14].

The key parameters to our method are the gain offset correlation coefficient K_{gain} , the offset residual error S_{off} , and the per-packet signal strength residual error S_{ss} . These

| Environment | K_{gain} | S_{off} (dB) | S_{ss} (dB) |
|---------------|-------------|----------------|---------------|
| Open Outdoor | 0.01 - 0.04 | 1.326 - 2.675 | 2.68 - 3.75 |
| Urban Outdoor | 0.15 - 0.19 | 2.244 - 3.023 | 2.46 - 2.75 |
| LOS Indoor | 0.25 - 0.38 | 2.837 - 5.242 | 2.9 - 5.28 |
| NLOS Indoor | 0.67 - 0.70 | 3.17 - 3.566 | 3.67 - 6.69 |

TABLE I: Summary of Data-Derived Simulation Parameters

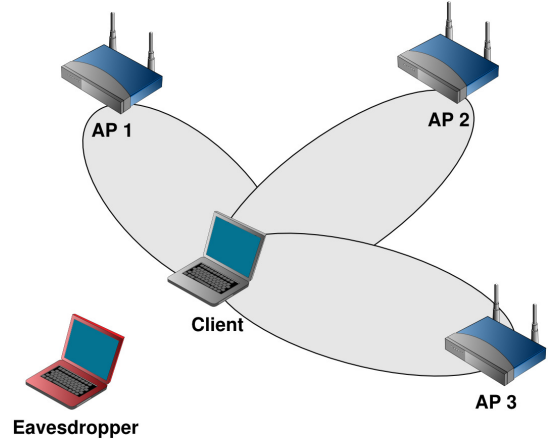


Fig. 3: Example of data stripping application

values were computed across many links for multiple environments. Table I summarizes these results. Importantly, similar environments produced similar values, even with different antennas. Because of this, it is possible for a researcher to select representative values based on a qualitative understanding of environment of interest.

EDAM’s principle of operation is that it generates randomized environmental effects based on the fitted distributions of effects measured in real environments. This has two main components: Algorithm (a) is a one-time initialization procedure which computes offsets between the antenna gain in any direction and the expected actual signal gain. Algorithm (b) computes the expected end-to-end gain for a given packet, *not including fixed path loss*. Thus, the simulated signal strength would be determined by the transmit power, path loss, receiver gain, fading model (if any), and the directional gain from Algorithm (a). Note that a fading model that accounts for inter-packet variation for stationary nodes may make the random error ϵ in line 9 redundant. In our simulation configurations below we refer to this error term as “implicit Gaussian” fading and consider scenarios where it is replaced with Ricean and Log-normal fading distributions.

IV. CASE STUDY: PHYSICAL SPACE SECURITY USING SMART ANTENNAS

In this section, we use the work of Lakshmanan et al. as a case study for the way antenna simulation strategy effects application layer performance. In [15], the authors propose “Data Striping” as a way of achieving physical space security by steering antennas. Downstream packets are encrypted and split into multiple parts so that all parts must be received in

Algorithm (a): Compute Directional Gain

```
1:  $K_{gain} \leftarrow$  gain offset correlation coefficient
2:  $S_{off} \leftarrow$  offset residual std. error
3: procedure DIRECT-GAIN
4:   for Node  $n \in$  all nodes do
5:      $P \leftarrow$  partition of azimuth range  $[-\pi, \pi)$ 
6:     for  $p_i \in P$  do
7:        $\theta_i \leftarrow$  center angle of  $p_i$ 
8:        $X \leftarrow$  random value ( $\mu = 0, \sigma^2 = S_{off}$ )
9:        $o_{n,p_i} \leftarrow K_{gain} * f_n(\theta_i) + X$ 
```

Algorithm (b): Compute Packet Gain

```
1:  $S_{pss} \leftarrow$  residual error of packet signal strengths
2: function DIRECTIONAL-PACKET-GAIN( $src, dst$ )
3:    $\theta_{src} \leftarrow$  direction from  $src$  toward  $dst$ 
4:    $\theta_{dst} \leftarrow$  direction from  $dst$  toward  $src$ 
5:    $p_{src} \leftarrow$  partition at  $src$  containing  $\theta_{src}$ 
6:    $p_{dst} \leftarrow$  partition at  $dst$  containing  $\theta_{dst}$ 
7:    $G_{src} \leftarrow f_{src}(\theta_{src}) - o_{dst,p_{src}}$ 
8:    $G_{dst} \leftarrow f_{dst}(\theta_{dst}) - o_{src,p_{dst}}$ 
9:    $\epsilon \leftarrow$  random value ( $\mu = 0, \sigma^2 = S_{pss}$ )
10:  return( $G_{src} + G_{dst} + \epsilon$ )
```

order to decode any portion of the packet. Several access points, which are presumed to have smart antennas, then transmit the packet-parts so that the only point at which all the required information is available is at the intended receiver. In this scenario (see figure 3), an eavesdropper who is outside the coverage area of *any* of the access points will only receive a subset of the packet parts and therefore be unable to reconstruct the message. The measure of the effectiveness is the size of the region in which an attacker can successfully receive and reconstruct packets for any given probability of success.

The authors verify their work using a custom simulator that implements the International Telecommunication Union’s (ITU) indoor attenuation model combined with log-normal fading. This channel model fits well with our discussion in Section II: while the path loss and fading models are nontrivial, there is no interaction between the environment and directionality. Because directionality is crucial to the proper function of this application, it is important to understand how the environment may affect performance.

A. Implementation

In order to understand the effects of the environment on the application and get a baseline for further analysis, we built a custom measurement testbed and ran tests in multiple environments - both indoors and outdoors. Figure 3 shows the conceptual layout of the experiments. Five nodes were used - three APs, one client, and one eavesdropper. The eavesdropper was positioned in many locations on a grid, at each of which the access points sent a volley of broadcast packets (approximately 500) to the client while the eavesdropper attempted to overhear them from its location. The indoor experiment was carried out in a cluttered office with 83 unique measurement points. The outdoor tests required 437 measurement points and were carried out in a large field on the University of Colorado campus.

All five nodes in the experiment were laptops running Linux, with Atheros radios. The access points used 24 dBi parabolic dish antennas, mounted on tripods and manually aimed at the client according to signal strength values. The client and eavesdropper used external omnidirectional antennas with approximately 5 dBi gain. For the indoor experiments, we reduced the power on the access points so that the

| Path Loss | Fading | Directivity Model |
|---------------------|---|--------------------------|
| Two-ray ITU 1238 | Log-normal Ricean Implicit Gaussian None | EDAM “Pure” “Omni” |

TABLE II: Physical-layer simulation options

received power at the (stationary) client was between -70 and -75 dBm. This was motivated by prior observations on the large amount of uncorrelated noise produced by high-power antennas in highly reflective indoor environments [16]. The outdoor experiments were carried out without any power reduction.

B. Simulation

For simulation, we used the popular network simulator QualNet 4.5 with physical layer simulations of varied complexity. Each configuration has some combination of the simulation layers listed in table II. We conducted a factorial experimental design, trying each unique combination of path loss model, directivity model, and fading model. While there are a variety of established path loss and fading models, we are not aware of any existing directivity models analogous to what we propose. The alternatives considered are essentially two null hypotheses: The first is that there is no significant environmental effect, and the antenna gain pattern sufficiently describes the signal directionality. This is the “*pure*” directivity model. The second is that environmental effects completely dominate the antenna effects, and so the signal is effectively isotropic. This is the “*omni*” directivity model. One might expect difficulty rejecting the first null hypothesis in an open outdoor environment, and the second in a highly-cluttered indoor environment.

The simulated experiments were modeled directly after the implementation discussed in section IV-A. Five nodes were simulated, placed in the same relative positions as in the actual experiments. The transmitters and intended receiver were stationary, while the eavesdropper moved to the same points as in the implementation. Both indoor and outdoor experiments were run. The simulation processes were identical except for the EDAM parameters: The indoor simulation used the

| Directivity Model | Vulnerability region (points) |
|--------------------------|-------------------------------|
| Measured | 38 |
| Pure antenna | 3 - 5 |
| EDAM | 54 - 79 |
| Omni (no directionality) | 83 (100%) |

TABLE III: Size of 50% vulnerability region, indoor scenario.

“non-line-of-sight (NLOS) indoor” values, while the outdoor simulation used the “urban outdoor” values. To deal with power calibration, we calibrated each simulation configuration manually so that the RSS values were comparable to those we observed in the actual implementation for only the intended receiver. We made ten unique runs per simulation, each with a different random seed.

C. Analysis

In alignment with the literature [1], our results show that system performance varies tremendously between simulation models. Table III shows the number of locations at which an eavesdropper can successfully decode $\geq 50\%$ of all packets. *The actual vulnerability region is 10 times what a current simulator would predict.*

By plotting the probability of an eavesdropper receiving a decodable packet at each position, we can observe that the simulations with the EDAM model is closer to reality than those without it. To quantify this effect, see figure 4 where a cumulative density function (CDF) of the probability of decoding a packet is plotted for each of the ten seeds against the measured data from the implementation. Looking at figures 4a and 4b, we can see that EDAM performs well. On the other hand, consider figures 4c and 4d, where state of the art models (such as those used here) without a directivity model grossly overestimate the effect of the antenna pattern on actual signal strength, and thus the performance of this application.

Figure 4e and 4f give plots of outdoor results. Figure 4e is a pathological case, with the “pure” directivity model and no fading model is used. In this case, the boundaries are stark - nearly 60% of locations are protected, while the remaining 40% are not. Although this performs poorly, it is worth considering as not all simulation software uses a fading model by default. For instance, the popular simulation package NS-2 does not unless it is paired with an extension such as [17]. Finally, figure 4f shows the best performing outdoor simulation strategy. We can see that the benefits of EDAM are more pronounced in indoor simulations where multipath reflections are more prevalent.

To determine which simulation approach produces application-layer results that are most consistent with the measured data, we compare the distribution of simulated application-layer performance with the distribution of actual performance. We use a two sample Kolmogorov-Smirnov (KS) test, which is effectively the maximal distance between the CDFs of the two samples. We then perform an analysis of variance (ANOVA) on the KS test results to determine

how much the various factors (directional model, path loss model, and fading model) contribute to the overall accuracy.

Figure 5 provides a box and whiskers plot of the KS test-statistic for each configuration. In this diagram lower values indicate better performance, meaning that the distribution of simulated performance closely follows the measured real-world performance. Alternately, high values indicate that the simulated performance deviates wildly from the measured performance. We can see that the configurations utilizing EDAM perform very well – producing application layer results which are much closer to reality than any other configuration. EDAM performs best in the indoor simulations, claiming the top three positions with this metric - EDAM with ITU 1238 and Ricean fading performs best, with less than 0.3 difference from the empirical data at maximum. The other two top positions are taken by EDAM with other fading or path loss models.

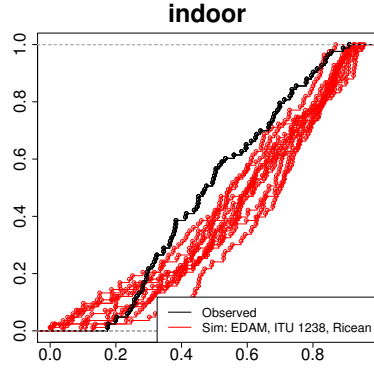
In the outdoor simulations, the conclusions are less strong - EDAM with Two-ray and Lognormal fading performs best, but is closely followed by EDAM with ITU 1238 and Ricean fading and Two-ray with Ricean fading and the “pure” directivity model. While the strength of EDAM is greatest in cluttered environments such as our indoor environment, it is important to note that it still offers a significant improvement in the outdoor environment.

Table IV shows the results of a factorial analysis of variance (ANOVA), using the KS statistic and the various physical layer simulation models as the factors. Note that the “omni” directivity model is not included because it is so inaccurate that its inclusion obscures the other effects. The test results show that the choice of directivity model is by far the dominant factor indoors, and a substantial factor outdoors.

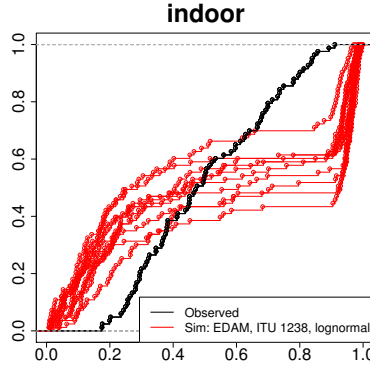
In the indoor environment, the effect of directivity model is *4.9 times greater than any other factor*. Outdoors, the path loss model is the dominant factor, followed by the fading model and then the directivity model. Both indoors and outdoors, a Ricean fading model performed better than log-normal or implicit Gaussian models. Somewhat predictably, the ITU 1238 indoor path loss model did better than the two-ray model indoors, but the two-ray model did better outdoors.

V. CONCLUSION

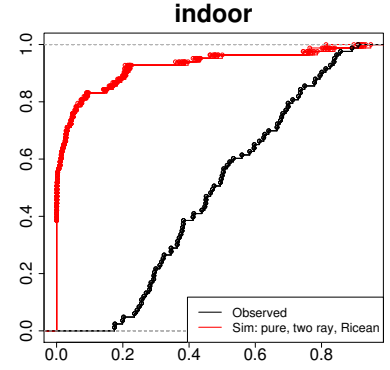
In this paper we have presented EDAM, a novel empirical method for improving the modeling of directional antennas in simulators. EDAM is both easy to implement and generalizable to a wide variety of directional antennas. We have shown that state of the art techniques for modeling physical-layer behavior for directional wireless networks can be misleading. Moreover, the addition of a directivity model to the conventional simulation stack provides a critical contribution to the ability of a simulator to produce realistic application layer results. *Not only do simulations using EDAM produce application layer results that are significantly more consistent with reality than traditional models in the application we study, but the choice of directivity model is the most influential factor in realistic simulation of indoor environments.* We have



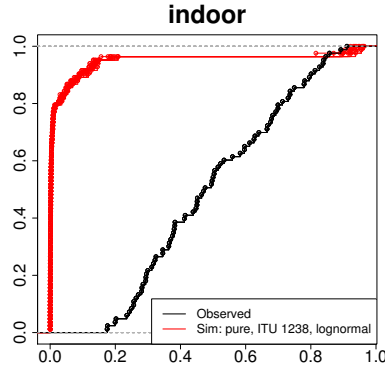
(a) EDAM, ITU 1238, Ricean fading, indoor



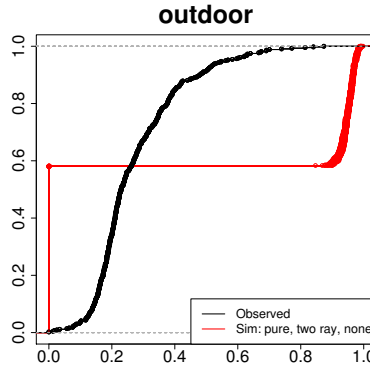
(b) EDAM, ITU 1238, Log-Normal fading, indoor



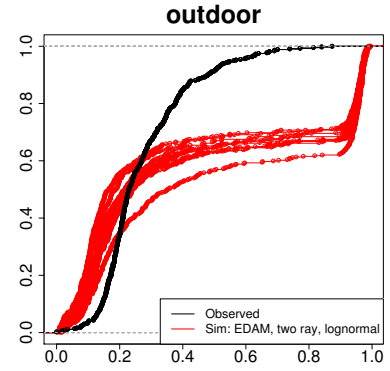
(c) Pure antenna model, Two-ray, Ricean fading, indoor



(d) Pure antenna model, ITU 1238, Log-normal fading, indoor



(e) Pure antenna model, Two-ray, no fading, outdoor



(f) EDAM, Two-ray, Log-normal fading, outdoor

Fig. 4: CDF plots of application layer performance for simulation configurations: The black line is the *observed data*, and the red (or grey) lines are the results of repeated simulation runs. The X axis is the proportion of decodable packets, and the Y axis is the cumulative fraction.

| Factor | Df | Indoor | | Outdoor | |
|--------------------------------------|----|----------|-----------|----------|---------|
| | | Mean Sq. | F-Value | Mean Sq. | F-Value |
| Dir. Model | 1 | 332.2 | 159911.55 | 27.14 | 34476 |
| P.L. Model | 1 | 68.0 | 32735.13 | 127.82 | 162367 |
| Fad. Model | 3 | 25.6 | 12315.35 | 73.46 | 93313 |
| Dir. Model * P.L. Model | 2 | 57.8 | 27841.84 | 31.49 | 39998 |
| Dir. Model * Fad. Model | 3 | 7.42 | 3572.82 | 27.70 | 35182 |
| P.L. Model * Fad. Model | 3 | 0.1 | 26.81 | 17.90 | 22733 |
| Dir. Model * P.L. Model * Fad. Model | 3 | 0.4 | 196.02 | 32.38 | 41135 |
| Error | | 0.0021 | | 0.001 | |

TABLE IV: Summary of results for factorial ANOVA on KS-test statistic across all simulation configurations except for the “omni” directivity model. P-values are omitted because all treatments are statistically significant at a level of $p < 2.2 * 10^{-16}$. Error / residual Df are 9948 indoor, 52428 outdoor.

KS-Test Statistic For all Configurations and Seeds

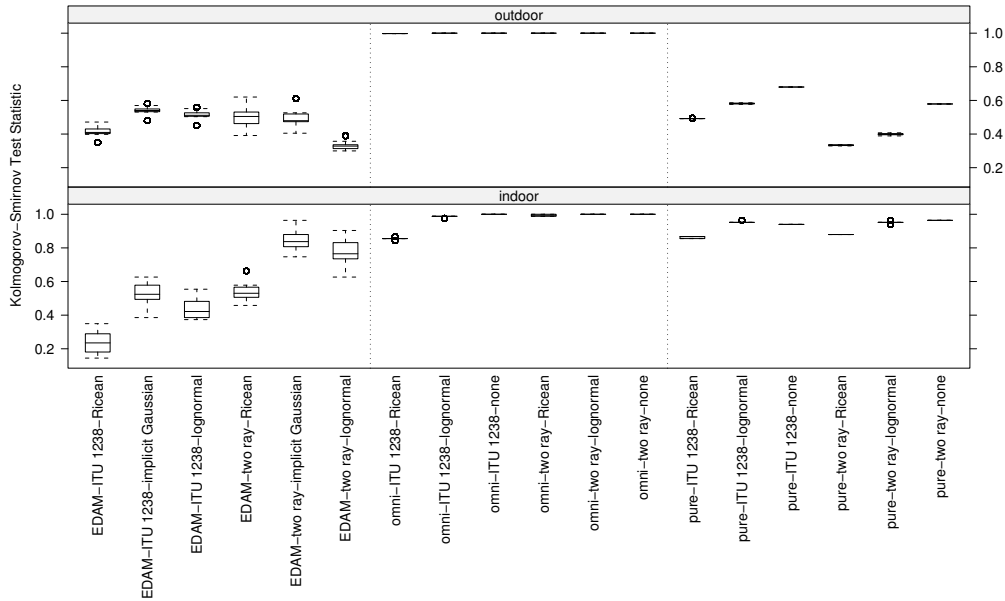


Fig. 5: Test-statistic of a two sample Kolmogorov-Smirnov test, run for each simulation configuration against the measured data (smaller values are better).

verified this with a factorial experimental design and a test-bed implementation in representative indoor and outdoor locations. EDAM is easily incorporated into wireless networking simulations¹, and is consistently more accurate than the state of the art for systems involving directional antennas.

REFERENCES

- [1] M. Takai, J. Martin, and R. Bagrodia, "Effects of wireless physical layer modeling in mobile ad hoc networks," in *MobiHoc '01: Proceedings of the 2nd ACM international symposium on Mobile ad hoc networking & computing*. New York, NY, USA: ACM, 2001, pp. 87–94.
- [2] V. Abhayawardhana, I. Wassell, D. C. , M. Sellars, and M. Brown, "Comparison of empirical propagation path loss models for fixed wireless access systems," in *Vehicular Technology Conference, 2005. VTC 2005-Spring. 2005 IEEE 61st*, vol. 1, no. 61. IEEE, June 2005, pp. 73–77.
- [3] C. Oestges and A. J. Paulraj, "Propagation into buildings for broad-band wireless access," *IEEE Transactions on Vehicular Technology*, vol. 53, no. 2, pp. 521 – 526, March 2004.
- [4] D. Green and A. Obaidat, "An accurate line of sight propagation performance model for ad-hoc 802.11 wireless LAN (WLAN) devices," in *Communications, 2002. ICC 2002. IEEE International Conference on*, vol. 5, 2002, pp. 3424 – 3428.
- [5] J. B. Andersen, T. S. Rappaport, and S. Yoshida, "Propagation measurements and models for wireless communications channels," *IEEE Communications Magazine*, vol. 33, no. 1, pp. 42 – 49, Jan 1995.
- [6] A. Neskovic, N. Neskovic, and G. Paunovic, "Modern approaches in modeling of mobile radio systems propagation environment," *IEEE Communications Surveys and Tutorials*, vol. 3, no. 3, 2000.
- [7] M. F. Iskander and Z. Yun, "Propagation prediction models for wireless communication systems," *IEEE Transactions on microwave theory and techniques*, vol. 50, no. 3, pp. 662 – 673, March 2002.
- [8] G. Wolffe, R. Wahl, P. Wertz, P. Wildbolz, and F. Landstorfer, "Deterministic propagation model for the prediction of hybrid urban and indoor scenarios," in *Personal, Indoor and Mobile Radio Communications, IEEE 16th International Symposium on (PIMRC)*, vol. 1, Sept. 2005, pp. 659 – 663.
- [9] R. Tingley and K. Pahlavan, "Space-time measurement of indoor radio propagation," *Instrumentation and Measurement, IEEE Transactions on*, vol. 50, no. 1, pp. 22 – 31, Feb 2001.
- [10] C. G. D. de Leon, M. Bean, and J. Garcia, "On the generation of correlated rayleigh envelopes for representing the variant behavior of the indoor radio propagation channel," in *Personal, Indoor and Mobile Radio Communications, 2004. PIMRC 2004. 15th IEEE International Symposium on*, vol. 4, Sept 2004, pp. 2757 – 2761.
- [11] E. Anderson, C. Phillips, G. Yee, D. Sicker, and D. Grunwald, "Modeling environmental effects on directionality in wireless networks," in *5th International workshop on Wireless Network Measurements (WiNMee)*, June 2009.
- [12] E. W. Zegura, K. Calvert, and S. Bhattacharjee, "How to model an internetwork," in *Infocom*. IEEE, 1996.
- [13] H. Tangmunarunkit, R. Govindan, S. Jamin, S. Shenker, and W. Willinger, "Network topology generators: degree-based vs. structural," in *SIGCOMM '02: Proceedings of the 2002 conference on Applications, technologies, architectures, and protocols for computer communications*. New York, NY, USA: ACM, 2002, pp. 147–159.
- [14] I. W. Lee and A. O. Fapojuwo, "Stochastic processes for computer network traffic modeling," *Computer Communications*, vol. 29, no. 1, pp. 1–23, December 2005. [Online]. Available: <http://www.sciencedirect.com/science/article/B6TYP-4FPN8DN-1/2/S3db1b14bee7d1c5eb734c479375ae3e>
- [15] S. Lakshmanan, C.-L. Tsao, R. Sivakumar, and K. Sundaresan, "Securing wireless data networks against eavesdropping using smart antennas," *ICDCS*, vol. 0, pp. 19–27, 2008.
- [16] E. Anderson, C. Phillips, D. Sicker, and G. Yee, "Modeling directionality in wireless networks [extended abstract]," in *ACM SigMetrics*, 2008.
- [17] N. Baldo, F. Maguolo, M. Miozzo, M. Rossi, and M. Zorzi, "ns2-miracle: a modular framework for multi-technology and cross-layer support in network simulator 2," in *ValueTools '07: Proceedings of the 2nd international conference on Performance evaluation methodologies and tools*. ICST, Brussels, Belgium, Belgium: ICST (Institute for Computer Sciences, Social-Informatics and Telecommunications Engineering), 2007, pp. 1–8.

¹Our implementation of EDAM for version 4.5 of the QualNet Simulator will be released at <http://systems.cs.colorado.edu/>